20th IMEKO TC4 International Symposium and
18th International Workshop on ADC Modelling and Testing
Research on Electric and Electronic Measurement for the Economic Upturn
Benevento, Italy, September 15-17, 2014

Calorimetric sensor to measure local calorific dissipations in the human body

Jesus[1] Ch., Socorro[1] F., Rodríguez de Rivera[1] M., Rodríguez de Rivera[2] H.J., Sarmiento[2] R.
[1]Departamento de Física (manuel.rguezderivera@ulpgc.es). [2]Departamento de Ingeniería Electrónica y Automática. Universidad de Las Palmas de Gran Canaria. 35017 Las Palmas de Gran Canaria. Spain.

***Abstract* – A calorimetric sensor for medical application has been developed in order to measure surface and localized calorific dissipations in the human body. The instrument tries to evaluate the calorific power that is transmitted by conduction, through a thermopile, between the human body and a thermostat at a constant temperature. The detection area of the prototype is 36 cm^2 and the sensor resolution is 50 mW. From the equations of heat transport by conduction, we propose a model based on the sensor decomposition in different domains connected to each other. The model is validated experimentally. The sensor operation domain is indicated and some practical applications to the human body are shown.**

I. INTRODUCTION

The calorimetric instrument which is shown has as an objective to measure surface and localized calorific dissipations in the human body. It involves measuring the power transmitted by conduction, through a thermopile, between the human body and a thermostat at a constant temperature. In this calorimetric application, the dissipation intended to be measured is not located inside the measuring instrument but outside, this is the reason why this instrument is out of the calorimetric standards [1]. However, an experimental prototype has been constructed and an operational method to measure the calorific power going through the sensor has been proposed. The operating principle is based on the Law of heat transfer by conduction and it can be included within the group of isothermal calorimeters as its operation requires a thermostat at a constant temperature [2].

These instrument applications are diverse because they will enable to study, in terms of power and energy, different energy processes developed in the human body. One of the possible applications is to control the power that is being dissipated when burning malignant cells with different processes. Another application is the measuring of the calorific dissipation in different parts of the human body surface: trunk, limbs, etc., in several activities. The prototype carried out has a capturing area of 36 cm^2 and it is valid for large surfaces. In previous works [3-4], different functions of the operation of this instrument have been presented. With this work, we intend to make a review explaining in detail its operation and indicating its most important characteristics, some experimental measures obtained in the human body will also be shown.

II. EXPERIMENTAL SYSTEM

The calorimetric sensor is mainly based on a thermopile (TEC1-12704 by Melcor of 40x40x5 mm) located between the thermostat and an aluminium plate (60x60x1 mm) that is leaned on the zone where the heat flux will be determined. By Seebeck effect, the thermopile provides the calorimetric signal. The thermostat is made up of a small aluminium block (40x40x5mm) that contains a heating resistance (R=50 Ω) and a RTD sensor; a cooling system based on another thermopile which, through Peltier effect, absorbs heat from the thermostat is also included within the thermostat; on the hot surface of this thermopile, an aluminium dissipator with its fan is attached. The whole device has a lateral thermal insulation. There is another RTD in the external part to measure the room temperature.

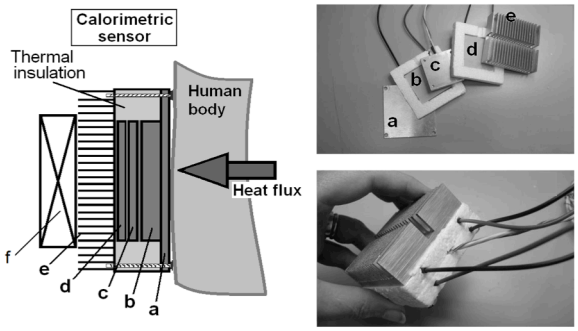

Fig. 1. Calorimetric sensor: a) aluminium plate, b) measuring thermopile, c) thermostat, d) cooling thermopile, e) aluminium dissipator f) fan

For the device calibration, a base consisting of an insulating box where the sensor is fitted has been constructed. This "calibration base" has a variable configuration depending on the required amount of calorific capacity of the copper sheet that contains the

ISBN-14: 978-92-990073-2-7

electrical resistance of Joule calibration. A power supply (Agilent E3631A) feeds the calibration resistance, the thermostat resistance and the cooling Peltier plate; the fan is feeded by another source. The calorimetric signal, the external and the thermostat temperatures are measured by a data acquisition system (Agilent 34970). The Agilent 82357B USB/GPIB Interface provides a direct connection from a USB port on our laptop to GPIB instruments. A MatLab program controls the experimental device, keeping constant the thermostat temperature through a PID controller and storing all the variables for its subsequent treatment. The sampling period is Δt =1 s.

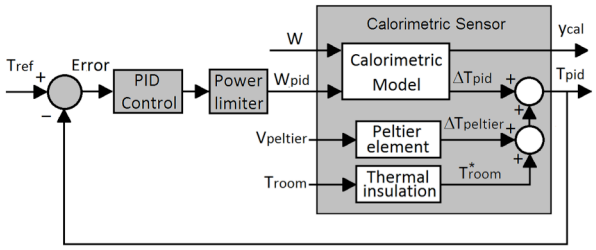

Fig. 2. Diagram of the calorimetric sensor calorimétrico

In order to explain the sensor operation, we show in Fig.2 a diagram of interconnected blocks in which it is included a close-loop control of the thermostat temperature, where T_{ref} is the intended thermostat temperature and T_{pid} is the real thermostat temperature. The PID controller determines the power W_{pid} to be dissipated in the thermostat. The PID controller parameters have been determined experimentally [5].

The block that represents the calorimetric sensor has been decomposed into three sub-blocks: the first one is the thermal insulation whose function is to integrate the room temperature T_{room}. The second block is the Peltier element whose function is to reduce the thermostat temperature if it is necessary. In the third block (calorimetric model), the inputs are the powers experienced by the sensor (W) and the one which is dissipated in the thermostat (W_{pid}), and the outputs are the calorimetric signal (y_{cal}) that provides the measuring thermopile and the increasing or reduction of the thermostat temperature (ΔT_{pid}). It is a multiple-input multiple-output system (MIMO). In stationary state, the fluctuations of the thermostat temperature, the calorimetric signal and the power dissipated in the thermostat are respectively: ± 0.01 K, ± 0.25 mV and ± 0.02 W.

The way in which this instrument operates is as follows: before a measurement in the human body, the sensor must be located on its base until it reaches the programmed thermostat temperature, afterwards, the sensor is applied on the zone of the human body that is intended to be measured and, when the thermostat temperature goes back to the stationary state, the sensor is again placed on its base. Before and/or after the measurement in the human body, when the sensor is on its base, the calibration measure is carried out by means of Joule effect.

Fig. 3. Positioning of the sensor on the human body

III. TWO-BODY MODEL

The modeling approach selected for the calorimeter is based on the localized-constant models [6]. Taking into account that the calorimetric signal depends on the temperatures of each measuring thermopile surface, we consider two bodies having these temperatures. The first one (C_1) represents the domain which covers the location where the dissipation takes place and one of the thermopile surfaces, and the second one (C_2) represents the domain made up by the thermostat and the other thermopile surface. Each body has a calorific capacity C_i and infinite thermal conductivity so that the temperature in all points of such element will be, theoretically, the same. Besides, each body is connected to one another, or to the outside, by means of thermal conductivity couplings P_{ik} (Fig.4).

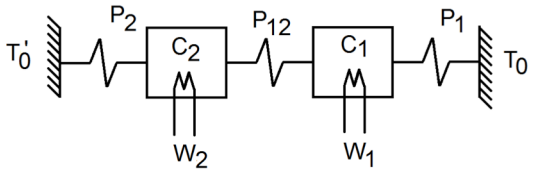

Fig.4. Calorimeter model.

The power developed in each domain is equal to the power to change its temperature plus the power transmitted by conduction to the adjacent domains:

$$W_1 = C_1 \frac{dT_1}{dt} + P_{12}(T_1 - T_2) + P_1(T_1 - T_0) \qquad (1)$$

$$W_2 = C_2 \frac{dT_2}{dt} + P_{12}(T_2 - T_1) + P_2(T_2 - T_0')$$

Supposing that the external temperatures T_0 and T'_0 are constant, the baselines of all time variables are corrected, and it is considered that the calorimetric output is proportional to the difference in temperatures:

$$Y_{cal} = k(T_1 - T_2) = k(\Delta T_1 - \Delta T_2) \quad (2)$$

Taking $W_1=W$, $W_2=W_{pid}$, $\Delta T_2=\Delta T_{pid}$, and applying the Laplace transform, we obtain Eq.3 which relates the inputs (W and W_{pid}) to the outputs (Y_{cal} and ΔT_{pid}).

$$\begin{pmatrix} TF_1 & TF_2 \\ TF_3 & TF_4 \end{pmatrix} \begin{pmatrix} W(s) \\ W_{pid}(s) \end{pmatrix} = \begin{pmatrix} Y_{cal}(s) \\ \Delta T_{pid}(s) \end{pmatrix} \quad (3)$$

In general, each TF_i has the form:

$$TF_i(s) = K_i \frac{(1 + s\tau_i^*)}{(1 + s\tau_1)(1 + s\tau_2)} \quad (4)$$

… K_i is the sensitivity, $\tau_i=-1/s_i$, $\tau_i^*=-1/s_i^*$, s_i and s_i^* are the poles and zeros. The four TF_i have the same poles, but the sensitivities and zeros are different.

For the model identification, we made a calibration that combines dissipations by Joule effect on the calibration base with programmed variations of the thermostat temperature of 24, 26 and 28 ºC on different calibration bases (Fig.5). The model parameters are determined by minimizing the mean squared error σ between the experimental curves and the curves calculated by the model. In order to do so, the simplex search algorithm method by Nelder and Mead [7] and the software MatLab [8] have been used.

$$\sigma = \sqrt{\frac{1}{N}\sum_{i=1}^{N}(y_{\exp}[i] - y_{cal}[i])^2} \quad (5)$$

… being N the number of dots of the experimental curve. Prior to the identification process, the input and output baselines are corrected. Table I shows the values of the model parameters. The change of the calibration base only affects the dynamic response through the value of C_1, but it does not alter the static response.

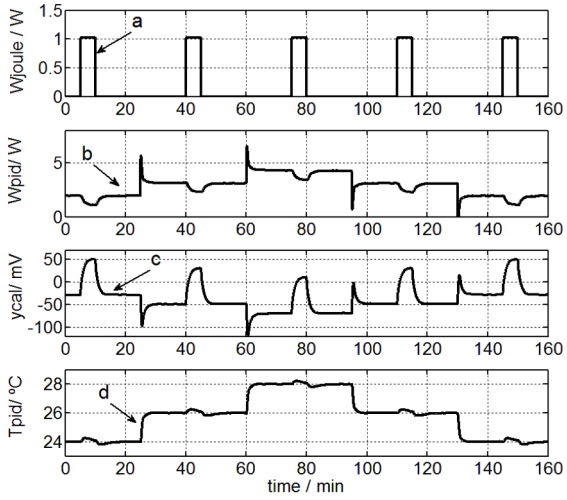

Fig. 5. Input and output signals used in the model: power dissipated in the calibration base (a) and in the thermostat (b), calorimetric signal (c) and thermostat temperature (d)

The average power, for a sensor application time t_d, is determined by means of the following equation:

$$W_{mean} = \frac{1}{t_d K_1}\left(\int y_{cal}(t)dt - K_2 \int W_{pid}(t)dt\right) \quad (6)$$

For the case shown in Fig.6, the areas are: Y_{cal} = 24.110 Vs, W_{pid} = -289.141 J. For t_d = 300 s, we obtain W_{mean}=1.014 W, being its experimental value 1.023 W. The result is independent from the time constants and the base selected for the calibration. The power is also determined by the relation:

$$\hat{W} = \frac{1}{TF_1} Y_{cal} - \frac{TF_2}{TF_1} W_{pid} \quad (7)$$

The noise is amplified by the derivative filters (Fig.6C) and it is necessary to apply a low-pass filter (Fig.6D) with cutoff frequency = 0.1 Hz (Nyquist frequency = 0.5 Hz). The mean squared error in the power determination is 44 mW.

Table I. Model parameters

RC Model		*TF Model*	
C_1	$32.37\ JK^{-1}$	K_1	$61.97\ mVW^{-1}$
C_2	$51.28\ JK^{-1}$	K_2	$-17.73\ mVW^{-1}$
P_1	$0.1434\ WK^{-1}$	K_3	$1.33\ KW^{-1}$
P_2	$0.5012\ WK^{-1}$	K_4	$1.62\ KW^{-1}$
P_{12}	$0.6562\ WK^{-1}$	τ_1	$133.5\ s$
K	$61.19\ mVK^{-1}$	τ_2	$25.2\ s$
		τ_1^*	$102.3\ s$
Errors (N=10000)		τ_2^*	$226.0\ s$
σ_y	$1.15\ mV$	τ_3^*	---
σ_T	$0.07\ K$	τ_4^*	$40.5\ s$

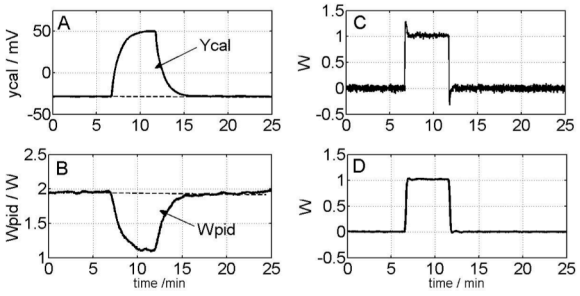

Fig.6 Calculation of the areas of the calorimetric signal Y_{cal} and of the thermostat power W_{pid}. Power calculated with the Eq 7 (curves C and D).

IV. OPERATING DOMAIN. APPLICATIONS.

By operating domain, we mean the margin of possible thermostat temperatures (T_{pid}) and the minimum detectable and the maximum calculable power.

As regards the margin of temperatures, this depends on the ambient temperature (T_{room}):

$$T_{pid} = T_{room} + \Delta T_{Peltier} + K_3 W + K_4 W_{pid} \qquad (8)$$

Initially, the following considerations are taken into account: there is no dissipation (W=0), $(\Delta T_{Peltier})_{max}$=0 K, $(\Delta T_{Peltier})_{min}$= -10 K, $(W_{pid})_{max}$= 8 W, so it is obtained: T_{room}-10 < T_{pid} < T_{room}+13. However, the right sensor operation requires that when there is dissipation W, the temperature control should not be saturated, this is the reason why, if a dissipation W_{max} is supposed, the limits for the thermostat temperature will be the following ones:

$$(T_{pid})_{max} = T_{room} + (\Delta T_{Peltier})_{max} + K_4 (W_{pid})_{max} - K_3 W_{max} \qquad (9)$$
$$(T_{pid})_{min} = T_{room} + (\Delta T_{Peltier})_{min} + K_4 (W_{pid})_{min} + K_3 W_{max}$$

Therefore, for W_{max}=1.5W, T_{room}-8 < T_{pid} < T_{room}+11.

The minimum detectable power is 10 mW, however, the results obtained in the deconvolution process provide squared errors of around 45 mW so we can say that the instrument resolution is 50 mW. The maximum power depends on the programmed temperature of the thermostat and the ambient temperature. At the limit, when W_{pid}=0, W_{max}= (T_{pid} -T_{room} - $\Delta T_{Peltier}$)/K_3

Finally, some measures carried out in the human body are presented. As an example, Fig. 7 shows an experimental measure carried out in the right pectoral zone of a healthy 22 year-old male subject in a sitting position, for a room temperature of 20.7 ºC. The deconvolution shows initial and final peaks due to positioning of the sensor and the transient due to the adaptation to the human body. The stationary state of the deconvolution, final zone of the curve in Fig7, allows to determine the power transmitted to the sensor. This deconvolution is carried out by means of a derivative filter [9] with a determined time constant so that the final part of the curve is made horizontal supposing that it tends towards a stationary state. In Fig.7, it is shown the filtering process with different time constants (τ = 0, 200, 400 and 600 s) obtaining the horizontal situations for τ=400 s. This filtering process amplifies the noise at high and low frequency, the latter is due to the oscillations of the ambient temperature. The time constant of the human body is far superior to the one of the base used in the calibration.

In Table II, measures in the pectoral zone for different thermostat temperatures are shown. It is evident that the greater the difference of temperatures between the thermostat and the human body, the higher the power should be. There are no references about this type of measures but we can say that, for these conditions, the dissipated powers are between 0.5 and 1.5 W [4].

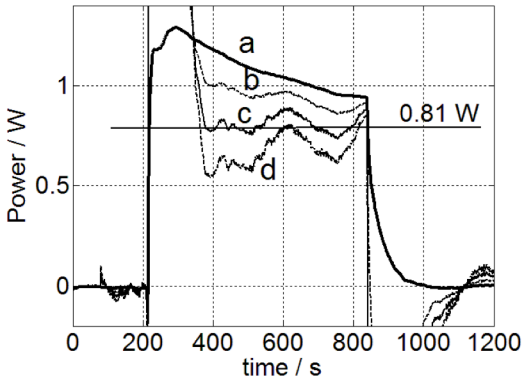

Fig.7. Power dissipated by the human body (right pectoral). Application of a derivative filter for τ=0 (a), τ=200 (b), τ=400 (c), τ=600 (d). T_{pid}=26ºC, T_{room}=20.7ºC.

Table II. Measures in the human body, healthy 22 year-old male subject in a sitting position (detection area of 36 cm^2).

Thermostat	*24.0 ºC*	*26.0 ºC*	*28.0 ºC*
Troom	*21.7 ºC*	*20.7 ºC*	*20.3 ºC*
Right pectoral	*1.10 W*	*0.81 W*	*0.70 W*
Left pectoral	*1.20 W*	*1.10 W*	*0.90 W*

V. CONCLUSIONS

A calorimetric sensor has been developed to measure surface and localized calorific dissipations in the human body. The modelization carried out from the equations of heat transport by conduction is adequate and it enables to reproduce and simulate the sensor operation perfectly. Besides, this modelization allows to study the way in which the constructive changes of the instrument affect the sensitivity.

The greatest difficulty of the thermal measures is the insulation of the process to be measured. This difficulty has been overcome to the limit determined by the sensor resolution, which is 50 mW in this prototype.

In the sensor calibration, a slightly different model is obtained for each calibration base in which it only changes the calorific capacity representing the dissipation place. This makes the dynamic response change but the static response remains constant; the sensitivities are independent from the base. A cooling thermopile enables to extend the operation margin of the sensor making it capable of taking measures in any reasonable environment.

Finally, it is necessary to point out that the measurements carried out in the human body are always dependent on the thermostat and the room temperatures, apart from the physical activity of the subject.

REFERENCES

[1] Handbook of Thermal Analysis and Calorimetry. Vol. 1. Principles and Practice. Ed. M.E. Brown, Elsevier Science (1998).

[2] Hansen LD. Toward a standard nomenclature for calorimetry. Thermochim Acta. 2001;371:19–22.

[3] Ch. Jesús, F. Socorro and M. Rodriguez de Rivera. Development of a calorimetric sensor for medical application. Part II. Identification and Simulation. J. Therm. Anal. Calorim. 2013; 113: 1003-1007.

[4] Ch. Jesús, F. Socorro and M. Rodriguez de Rivera. Development of a calorimetric sensor for medical application. Part III. Operating methods and applications. J. Therm. Anal. Calorim. 2013; 113: 1009-1013

[5] Goodwin GC, Graebe SF, Salgado ME. Control System Design. Prentice Hall. New Jersey, 2001.

[6] Socorro F, Rodríguez de Rivera M, Jesús Ch. A thermal model of a flow calorimeter. J Therm Anal Calorim. 2001;64:357–66.

[7] Nelder JA, Mead C. A simplex method for function minimization. Comput J. 1965;7:308–13.

[8] The MathWorks, Inc. Optimization ToolboxTM User's Guide, 5th printing. Revised for Version 3.0 (Release 14), June 2004.

[9] Marco F, Rodríguez de Rivera M, Ortin J, Serra T, Torra V. A frecuential analysis of the numerical algorithms used for inverse filtering in calorimetry. Thermochim. Acta. 1986; 102: 173-178.